

In Vitro and *In Vivo* Metabolic Studies of Phospho-aspirin (MDC-22)

Gang Xie · Chi C. Wong · Ka-Wing Cheng · Liqun Huang · Panayiotis P. Constantinides · Basil Rigas

Received: 26 March 2012 / Accepted: 22 June 2012 / Published online: 11 July 2012
© Springer Science+Business Media, LLC 2012

ABSTRACT

Purpose To investigate the metabolism of phospho-aspirin (PA, MDC-22), a novel anti-cancer and anti-inflammatory agent.

Methods The metabolism of PA was studied in the liver and intestinal microsomes from mouse, rat and human.

Results PA is rapidly deacetylated to phospho-salicylic acid (PSA), which undergoes regioselective oxidation to generate 3-OH-PSA and 5-OH-PSA. PSA also can be hydrolyzed to give salicylic acid (SA), which can be further glucuronidated. PA is far more stable in human liver or intestinal microsomes compared to those from mouse or rat due to its slowest deacetylation in human microsomes. Of the five major human cytochrome P450 (CYP) isoforms, CYP2C19 and 2D6 are the most active towards PSA. In contrast to PSA, conventional SA is not appreciably oxidized by the CYPs and liver microsomes, indicating that PSA is a preferred substrate of CYPs. Similarly, PA, in contrast to PSA, cannot be directly oxidized by CYPs and liver microsomes, indicating that the acetyl group of PA abrogates its oxidation by CYPs.

Conclusions Our findings establish the metabolism of PA, reveal significant inter-species differences in its metabolic transformations, and provide an insight into the role of CYPs in these processes.

KEY WORDS cytochrome P450 · glucuronidation · liver microsomes · phospho-aspirin · regioselective oxidation

ABBREVIATIONS

| | |
|-----|--------------------------------|
| ASA | acetylsalicylic acid (aspirin) |
| CES | carboxylesterases |
| CYP | cytochrome P450 |
| DFP | diisopropyl fluorophosphate |
| HLM | human liver microsomes |
| MLM | mouse liver microsomes |
| RLM | rat liver microsomes |
| PA | phospho-aspirin |
| PSA | phospho-salicylic acid |
| SA | salicylic acid |

INTRODUCTION

Aspirin (acetylsalicylic acid, ASA) is the most commonly used non-steroidal anti-inflammatory drug for relieving pain, inflammation and fever (1). ASA also reduces the risk of various cancers including those of colon, stomach, lung and breast (2). While it was originally thought that ASA suppressed carcinogenesis *via* the inhibition of cyclooxygenase-2 (COX-2), recent studies revealed that COX-independent mechanisms are also involved (3). For example, ASA inhibits tumor growth by directly inducing apoptosis in cancer cells through alteration of the Mcl-1/Noxa balance (4), and suppresses tumor angiogenesis by reducing angiogenic factor secretion by cancer cells (5).

Chemoprevention of cancer requires long-term drug prescription in otherwise healthy individuals and thus drug safety is paramount. Although widely used, ASA is not risk-free; it increases the risk of hemorrhagic stroke and gastrointestinal bleeding (6,7). Mechanistically, ASA covalently modifies and

G. Xie · C. C. Wong · K.-W. Cheng · L. Huang · B. Rigas (✉)
Stony Brook University, Division of Cancer Prevention
HSC, T17-080
Stony Brook, New York 11794-8175, USA
e-mail: basil.rigas@stonybrook.edu

P. P. Constantinides
Medicon Pharmaceuticals, Inc.
Stony Brook, New York 11790, USA

inactivates COX, thus reducing prostaglandin synthesis (8). These considerations prompted us to chemically modify ASA at its $-\text{COOH}$ group to generate phospho-aspirin (PA, MDC-22), which consists of ASA to which two diethylphosphate groups are covalently bound *via* a glycerol spacer (Fig. 1a). Indeed, PA is highly efficacious in the treatment of cancer and arthritis in preclinical animal models, and shows much less gastrointestinal toxicity than ASA (9,10).

Drug metabolism plays a key role in defining the efficacy and toxicity of drugs. Preclinical data on differences in drug metabolism between animals and humans help predict pharmacological outcomes in humans. Here, we investigated the metabolism of PA *in vitro* and *in vivo*. In addition to defining its major metabolic pathways, our results reveal significant interspecies differences in PA metabolism, and provide an insight into the interactions of PA and its metabolites with human cytochrome P450s (CYPs).

MATERIALS AND METHODS

Reagents

PA was provided by Medicon Pharmaceuticals, Inc. (Stony Brook, NY). 3-OH-SA, 5-OH-SA, ASA acyl glucuronide, SA phenolic glucuronide and diisopropyl fluorophosphate were purchased from Toronto Research Chemicals (Toronto,

Canada). ASA, SA, porcine liver esterases were purchased from Sigma-Aldrich (St. Louis, MO). SA acyl glucuronide was purchased from LC Scientific Inc. (Concord, ON, Canada). Mouse, rat and human liver microsomes, NADPH regenerating solution and UGT reaction solution were purchased from BD Biosciences (San Jose, CA). Mouse, rat and human intestinal microsomes, and mouse hepatocytes were purchased from XenoTech LLC (Lenexa, KS).

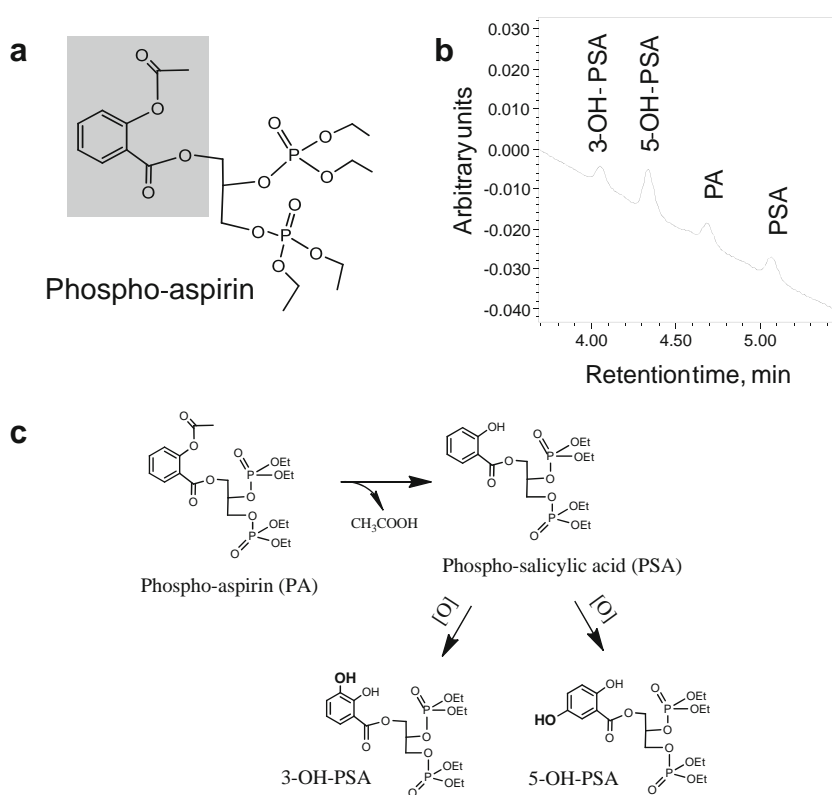
HPLC-UV Analysis

The HPLC system consisted of a Waters Alliance 2695 Separations Module equipped with a Waters 2998 photodiode array detector (236 nm) and a Thermo Hypersil BDS C18 column (150×4.6 mm, particle size 3 μm). The mobile phase consisted of a gradient between aqueous phase (Trifluoroacetic acid, CH_3CN , H_2O [0.1:4.9:95 v/v/v]) and CH_3CN at a flow rate of 1 ml/min at 30°C. A gradient elution from 0% to 100% CH_3CN from 0 to 15 min was applied and maintained at 100% CH_3CN until 18 min.

LC-MS/MS Analysis

The LC-MS/MS system consisted of Thermo TSQ Quantum Access (Thermo-Fisher, San Jose, CA) triple quadrupole mass spectrometer interfaced by an electrospray ionization probe with an Ultimate 3000 HPLC system (Dionex Corporation,

Fig. 1 Metabolism of PA by liver microsomes. **(a)** The structure of PA is shown; the shaded part of the molecule corresponds to the conventional aspirin. **(b)** HPLC chromatogram of an extract of rat liver microsomes incubated with PA for 30 min. **(c)** Major metabolic pathway of PA in liver microsomes.



Sunnyvale, CA). Chromatographic separations were achieved on a Luna C18 column (150×2 mm), and the mobile phase consisted of a gradient from 10% to 95% CH₃CN.

Phase I Metabolism of PA in Liver and Intestinal Microsomes

PA was pre-incubated at 37°C for 5 min with NADPH-regenerating solution (1.3 mM NADP, 3.3 mM D-glucose 6-phosphate, 3.3 mM MgCl₂, and 0.4 U/ml glucose-6-phosphate dehydrogenase) in 0.1 M potassium phosphate buffer (pH 7.4). The reaction was initiated by the addition of liver microsomes (protein concentration 0.5 mg/ml) or intestinal microsomes (protein concentration 0.25 mg/ml) and samples were maintained at 37°C for various time periods. At the end of the incubation, 0.1-ml aliquots were mixed with 0.2 ml of CH₃CN, vortexed and centrifuged for 10 min at 13,000 × g. The supernatants were subjected to HPLC analysis. The HPLC peaks corresponding to each metabolite were collected, and subjected to LC-MS/MS analysis.

To determine the kinetic parameters for PA metabolites formed in liver microsomes, PA was studied in serial dilutions from 400 to 4 μM. PA at each concentration was incubated with 0.5 mg/ml liver microsomes at 37°C for 10 min. After extraction with CH₃CN, the metabolites of PA were analyzed by HPLC. The kinetic parameters K_m and V_{max} were obtained using GraphPad Prism version 5.0.

Metabolism of PA by Mouse Hepatocytes

Cryopreserved mouse hepatocytes were thawed and incubated following the manufacturer's protocol. Briefly, hepatocytes were incubated with PA in 24-well tissue culture plates at a density of 2.5×10^5 cells/well in 5% CO₂ at 37°C. At the designated time-points, the cells were mixed with 2-fold volume of acetonitrile to stop the reaction. After centrifugation, the supernatants were analyzed by HPLC.

Stability of PA in Liver and Intestinal Microsomes

The half-life ($t_{1/2}$) of PA was determined by non-linear regression analysis in a one-phase decay model using GraphPad Prism version 5.0. Intrinsic clearance (CL_{int}) of PA was calculated using the formula $CL_{int} = (0.693/t_{1/2}) \times (V/P)$, where V is the incubation volume, and P is the mass of microsomal proteins in the incubation mixture (11).

The Metabolism of PSA by Human CYP Isoforms

PSA was pre-incubated at 37°C for 5 min with an NADPH-regenerating solution in 0.1 M potassium phosphate buffer (pH 7.4). The reaction was initiated by the addition of individual recombinant human CYP isoforms (25 pmol/ml) in a

total volume of 1 ml and samples were maintained at 37°C for various time periods. At each designated time-point, an aliquot was mixed with a 2-fold volume of CH₃CN, vortexed and centrifuged for 10 min at 13,000 × g. The supernatants were subjected to HPLC analysis.

Glucuronidation of PA by Liver Microsomes

PA was pre-incubated at 37°C for 5 min with UGT reaction solution (UDP glucuronic acid 2 mM, alamethicin 25 μg/ml and MgCl₂ 8 mM) in 50 mM Tris-HCl buffer (pH 7.5). The reaction was initiated by the addition of liver microsomes (protein concentration 0.5 mg/ml) and samples were maintained at 37°C for various time periods. At each designated time point, aliquots were mixed with 2-fold volume of CH₃CN, vortexed, and then centrifuged for 10 min at 13,000 × g. The supernatants were then subjected to HPLC analysis.

Metabolism of PA in Rats

Rats were administered orally by gavage equimolar PA or ASA (0.2 mmol/kg) in corn oil and were sacrificed 1 h post-dosing. Blood from the sacrificed animals was collected and immediately centrifuged. The resulting plasma was deproteinized by immediately mixing it with a 2-fold volume of CH₃CN, and the supernatants were subjected to HPLC analysis.

Statistical Analysis

Results were analyzed using the Student's *t*-test; $p \leq 0.05$ was considered statistically significant.

RESULTS

Phase I Metabolism of PA by Liver Microsomes and Hepatocytes

Initially, we explored and compared the metabolism of PA by mouse liver microsomes (MLM), rat liver microsomes (RLM) and human liver microsomes (HLM). Three major metabolites of PA (phospho-salicylic acid [PSA], 3-OH-PSA and 5-OH-PSA) are readily detected in PA-treated liver microsomes (Fig. 1b). This result indicates that PA can be readily deacetylated at its ASA moiety to form PSA, which undergoes regioselective oxidation to form 3-OH-PSA and 5-OH-PSA (Fig. 1c).

The metabolites were identified by LC-MS/MS analysis (Fig. 2). The mass spectrum of PSA showed a $[M+Na]^+$ ion at m/z 507, which was further fragmented to generate m/z 387 and 353 (Fig. 2). The mass spectrum of both 3-OH-PSA

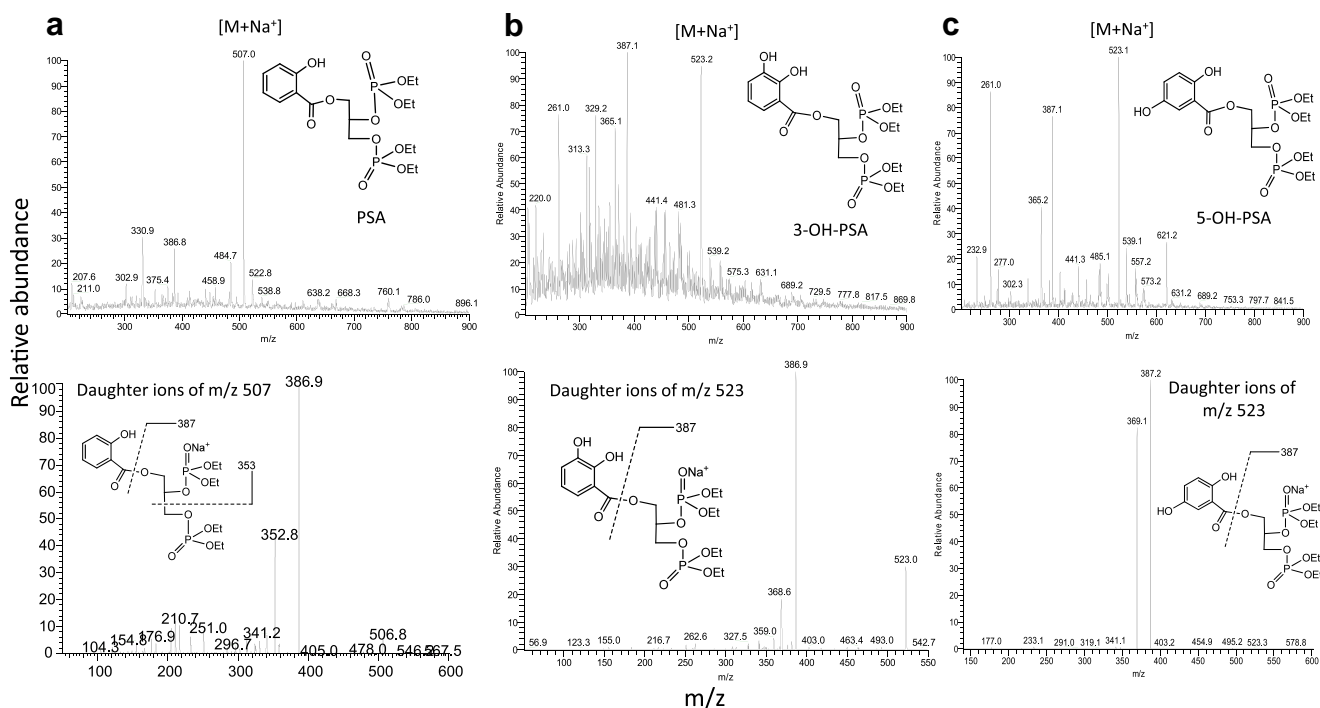


Fig. 2 Identification of PA metabolites by liver microsomes. **(a)** Top, MS spectrum of PSA. Bottom, MS/MS spectrum of the major fragments of PSA ion. **(b)** Top, MS spectrum of 3-OH-PSA. Bottom, MS/MS spectrum of the major fragments of 3-OH-PSA ion. **(c)** Top, MS spectrum of 5-OH-PSA. Bottom, MS/MS spectrum of the major fragments of 5-OH-PSA ion.

and 5-OH-PSA showed a $[M+Na]^+$ ion at m/z 523. This ion was fragmented at its carboxylic ester bond to generate m/z 387, which further generated m/z 369 upon loss of a water molecule. The position of the $-OH$ group in 3-OH-PSA and 5-OH-PSA was determined by treatment with porcine liver esterases, which hydrolyzed 3-OH-PSA and 5-OH-PSA to release 3-OH-SA and 5-OH-SA, respectively.

The level of PA in liver microsomes decreased rapidly due to its rapid deacetylation to form PSA (Fig. 3a). Five minutes after the reaction, 29%, 56% and 68% of PA was deacetylated by human, rat and mouse liver microsomes, respectively, indicating that the deacetylation rate of PA by liver microsomes increased in the order: human < rat < mouse. As a result, PA was by far the most stable in HLM as evidenced by its longest half-life ($t_{1/2}$) and slowest intrinsic clearance (CL_{int}) in HLM (Table I). We also determined the kinetic parameters of the major metabolites of PA by liver microsomes (Table II). These data support that the deacetylation of PA, regardless of the species, is the most efficient reaction in PA metabolism by liver microsomes.

The levels of the 3-OH-PSA and 5-OH-PSA generated in HLM were much lower than those in MLM and RLM during the entire period of observation (Fig. 3a), indicating that the oxidation of PSA is the slowest in HLM. PSA displayed a similar kinetic behavior in MLM and RLM: its level reached peak value within ~ 5 min, and subsequently decreased due to its rapid oxidation. In contrast, the level of

PSA increased continuously in HLM (Fig. 3a), reflecting the slow deacetylation of PA and the slow oxidation of PSA in HLM.

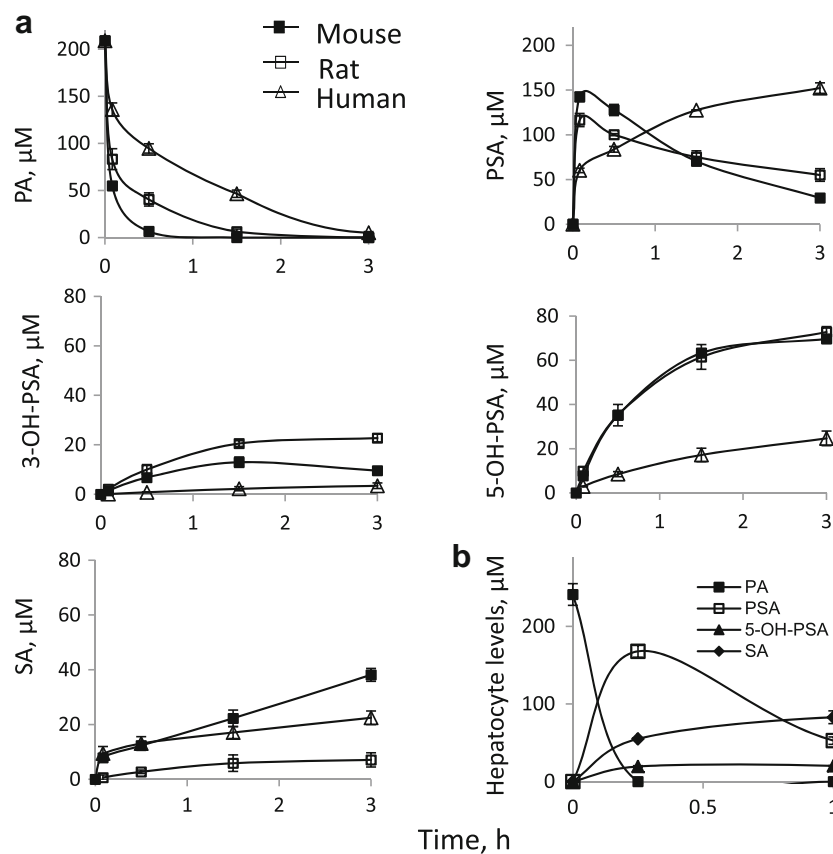
PSA, 3-OH-PSA and 5-OH-PSA also can be further hydrolyzed at their carboxylic ester bond (which links an SA moiety to a glycerol phosphate moiety) to give salicylic acid (SA), 3-OH-SA and 5-OH-SA, respectively. Twenty hours after the reaction, the hydrolysis of PSA, 3-OH-PSA and 5-OH-PSA was essentially complete in MLM; whereas the majority of these metabolites are still present in HLM and RLM, indicating that the carboxylesterase activity is the highest in MLM.

In contrast to PSA, conventional SA and ASA were not appreciably oxidized by liver microsomes of the three species under the same experimental conditions, indicating that PSA is a preferred substrate of the oxidative enzymes compared to conventional SA and ASA.

To determine whether PA can be directly oxidized by liver microsomes, we pre-treated MLM with diisopropyl fluorophosphate (DFP) at 200 μ M to abrogate its esterase activity, and evaluated the oxidation of PA *versus* PSA by DFP-treated MLM. In contrast to PSA, PA was not appreciably metabolized. Thus, PA cannot be directly oxidized by liver microsomes, and deacetylation of PA to PSA is required for its subsequent oxidation by liver microsomes.

We also examined the metabolism of PA by mouse hepatocytes. Similar to the case with liver microsomes, PA was

Fig. 3 Kinetics of PA metabolism by liver microsomes and hepatocytes. **(a)** Timecourses of the levels of PA and its metabolites formed in liver microsomes from mouse, rat or human. PA at 200 μM was incubated with liver microsomes and an NADPH-regenerating solution at 37°C for up to 3 h. PA and its metabolites were extracted at the designated time points and assayed as described in Methods. **(b)** Time-course of the levels of PA and its metabolites formed in mouse hepatocytes.



rapidly deacetylated to form PSA, which was subsequently oxidized and hydrolyzed to give 5-OH-PSA and SA, respectively (Fig. 3b). Minimal levels of 3-OH-PSA were also detected (not shown).

Phase I Metabolism of PA in Intestinal Microsomes

Since the small intestine also plays an important role in the first-pass metabolism of orally ingested xenobiotics (12), we next examined the metabolism of PA by the intestinal microsomes from mouse, rat and human. PA was rapidly deacetylated to form PSA, which undergoes oxidation and hydrolysis reactions to form 5-OH-PSA and SA, respectively (Fig. 4). 3-OH-PSA was undetectable in PA-treated intestinal microsomes. PA was by far the most stable in human intestinal microsomes among the three species as evidenced

by its longest $t_{1/2}$ and slowest CL_{int} (Table I). All three metabolic reactions (deacetylation, hydrolysis and oxidation) are much slower in intestinal microsomes compared to those in liver microsomes, and thus, PA was far more stable in intestinal microsomes than in liver microsomes (Table I).

Glucuronidation of PA in Liver Microsomes

Glucuronidation is an important phase II conjugation for most NSAIDs. We examined the metabolism of PA in the presence of UDP-glucuronic acid in liver microsomes. PA was deacetylated to form PSA, which was further hydrolyzed to form SA (Fig. 5a). The resulting SA was glucuronidated at its $-\text{COOH}$ and phenolic $-\text{OH}$ group to form its acyl and phenolic glucuronide, respectively, with the former being more abundant (Fig. 5b).

Since NADPH was not present in this reaction system, there was no oxidation of PSA. Regardless of the presence of NADPH, the stability of PA in liver microsomes decreased in the order: human > rat > mouse (Fig. 5a). The level of PSA plateaued after it reached its peak value at ~ 5 min in RLM and HLM. In contrast, PSA level decreased markedly during the same period of time in MLM (Fig. 5a), reflecting the rapid hydrolysis of PSA to SA in MLM.

To determine whether PA can be directly glucuronidated, we evaluated the glucuronidation of PA in DFP-

Table I The Stability ($t_{1/2}$ and CL_{int}) of PA in the Liver and Intestinal Microsomes from Mouse, Rat and Human

| | Liver | | Intestine | |
|-------|----------------------|----------------------------|----------------------|----------------------------|
| | $t_{1/2}/\text{min}$ | $CL_{int}/\text{ml/min/g}$ | $t_{1/2}/\text{min}$ | $CL_{int}/\text{ml/min/g}$ |
| Mouse | 2.4 | 567 | 199 | 14 |
| Rat | 3.2 | 433 | 119 | 23 |
| Human | 28.2 | 49 | 486 | 6 |

Table II Kinetic Parameters for the Metabolites of PA Generated in Liver Microsomes from Mouse, Rat and Human

| Metabolite | Mouse | | | Rat | | | Human | | |
|------------|------------------|--------------------------|---------------------------|------------------|--------------------------|---------------------------|------------------|--------------------------|---------------------------|
| | K_m μM | V_{max} pmol/mg/min | V_{max}/K_m ml/g/min | K_m μM | V_{max} pmol/mg/min | V_{max}/K_m ml/g/min | K_m μM | V_{max} pmol/mg/min | V_{max}/K_m ml/g/min |
| PSA | 77 | 32,820 | 426 | 122 | 39,720 | 326 | 95 | 9,320 | 98 |
| 5-OH-PSA | 17 | 1,360 | 80 | 9 | 1,720 | 185 | 46 | 620 | 13 |
| SA | 3 | 420 | 140 | Not Detected | | | 2 | 64 | 38 |

treated MLM. As shown in Fig. 5c, the hydrolysis of PA was abrogated by DFP, and no glucuronide metabolites were detected; in contrast, SA was glucuronidated to form its acyl and phenolic glucuronides. Thus, the presence of free phenolic -OH and -COOH group in SA are required for its phenolic and acyl glucuronidation, respectively.

Regioselective Oxidation of PSA by Human CYPs

Given the significant oxidation of PSA in liver and intestinal microsomes that contain a full complement of cytochrome P450s (CYPs), we evaluated PSA oxidation by five major human CYPs. CYP 2C19 and 2D6 were the most active towards PSA, whereas CYP1A2 was inactive (Fig. 6). In contrast to PSA, conventional SA and ASA were not appreciably oxidized by the human CYPs under

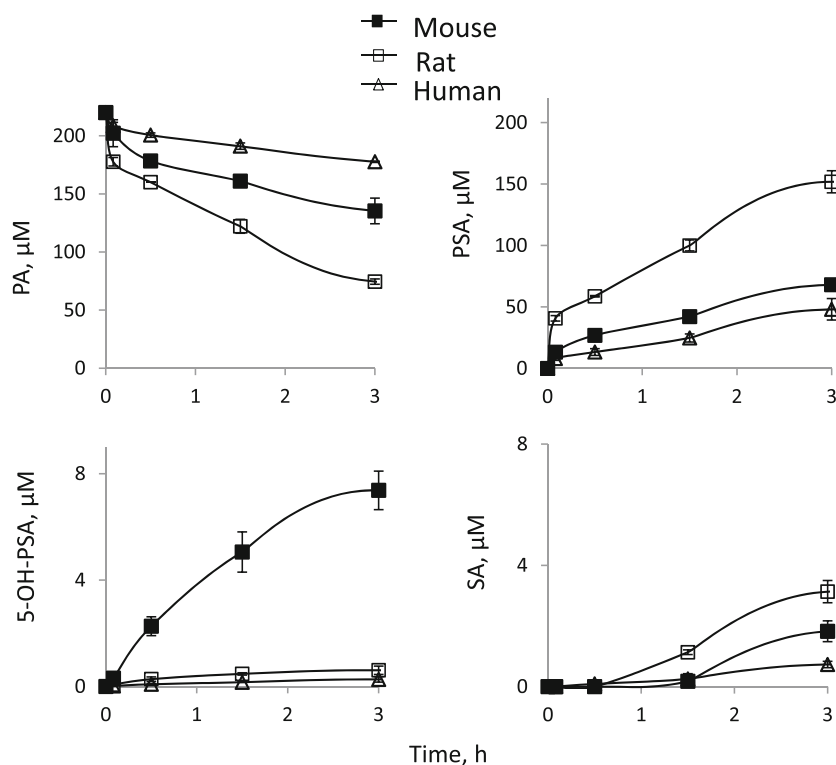
the same experimental conditions, indicating that PSA is the preferred substrate of CYPs. This result is consistent with our observation that SA or ASA was not oxidized in liver microsomes.

The Metabolism of PA in Rats

We administered orally equimolar amounts of PA or ASA to rats, and sacrificed them 1 h post-dosing. The only metabolite detected in the rat plasma was SA. The striking difference in PA metabolite profile *in vivo* and *in vitro* reflects the high abundance of carboxylesterases in rats. Similar to our finding, a nitric oxide derivative of ASA generated SA as its only detectable metabolite in rat plasma (13).

Interestingly, ASA generated 3.1 times higher SA level in rat plasma than PA, with their difference being statistically significant ($P < 0.01$; Fig. 7). This result is consistent with our

Fig. 4 Kinetics of PA metabolism by intestinal microsomes. Levels of PA and its metabolites as a function of time in PA-treated intestinal microsomes of mouse, rat or human. PA at 200 μM was incubated with intestinal microsomes and NADPH-regenerating solution at 37°C for up to 3 h. PA and its metabolites were extracted at the designated time points and assayed as described in Methods



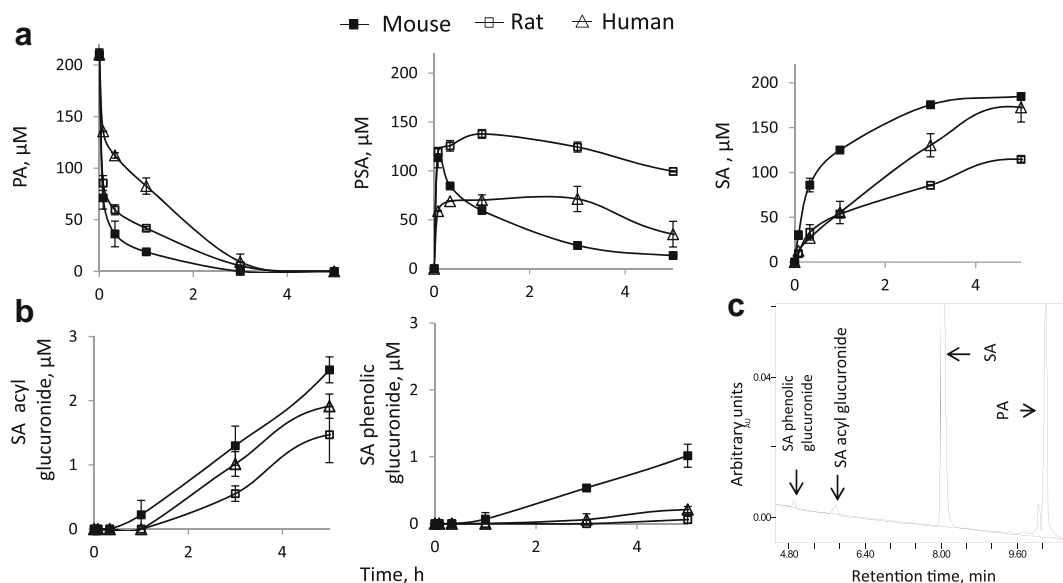


Fig. 5 Glucuronidation reactions of PA by liver microsomes. **(a)** Levels of PA and its hydrolysis metabolites as a function of time in PA-treated liver microsomes of mouse, rat or human. PA at 200 μM was incubated with liver microsomes and UDP-glucuronic acid at 37°C for up to 5 h. PA and its metabolites were extracted at the designated time points and assayed as described in Methods. **(b)** Time course of the levels of SA glucuronides in PA-treated liver microsomes. **(c)** HPLC chromatogram of the glucuronidation of PA (dotted line) or SA (solid line) in DFP-treated MLM 1 h after the reaction.

previous observations that phospho-compounds generate lower drug levels in plasma compared to their parent compounds (14,15), suggesting that this is a common feature of this class of compounds.

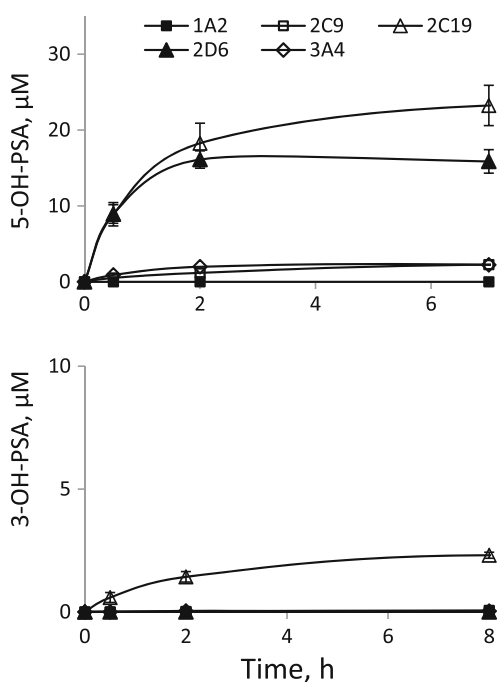


Fig. 6 Oxidation kinetics of PSA by human CYP isoforms. PSA at 200 μM was incubated with individual human CYP isoforms and NADPH-regenerating solution at 37°C for up to 7 h. The oxidized products were extracted at the designated time points and assayed by HPLC.

DISCUSSION

The present study establishes the metabolic pathways of PA. As illustrated in Fig. 8, PA undergoes the following metabolic reactions: 1) *deacetylation* at its ASA moiety to form PSA; 2) *regioselective oxidation* of PSA to form 3-OH-PSA and 5-OH-PSA; 3) *hydrolysis* of the carboxylic ester bond in PA, PSA, 3-OH-PSA and 5-OH-PSA to give the corresponding free acids; and 4) *glucuronidation* of ASA and SA to form glucuronide conjugates.

An important chemical feature of PA is the presence of two ester bonds, an acetyl ester bond and a carboxylic ester bond. Their hydrolysis has profound pharmacological significance, as the breakdown of PA to its individual

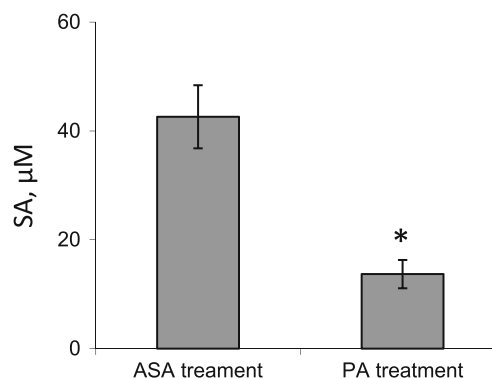
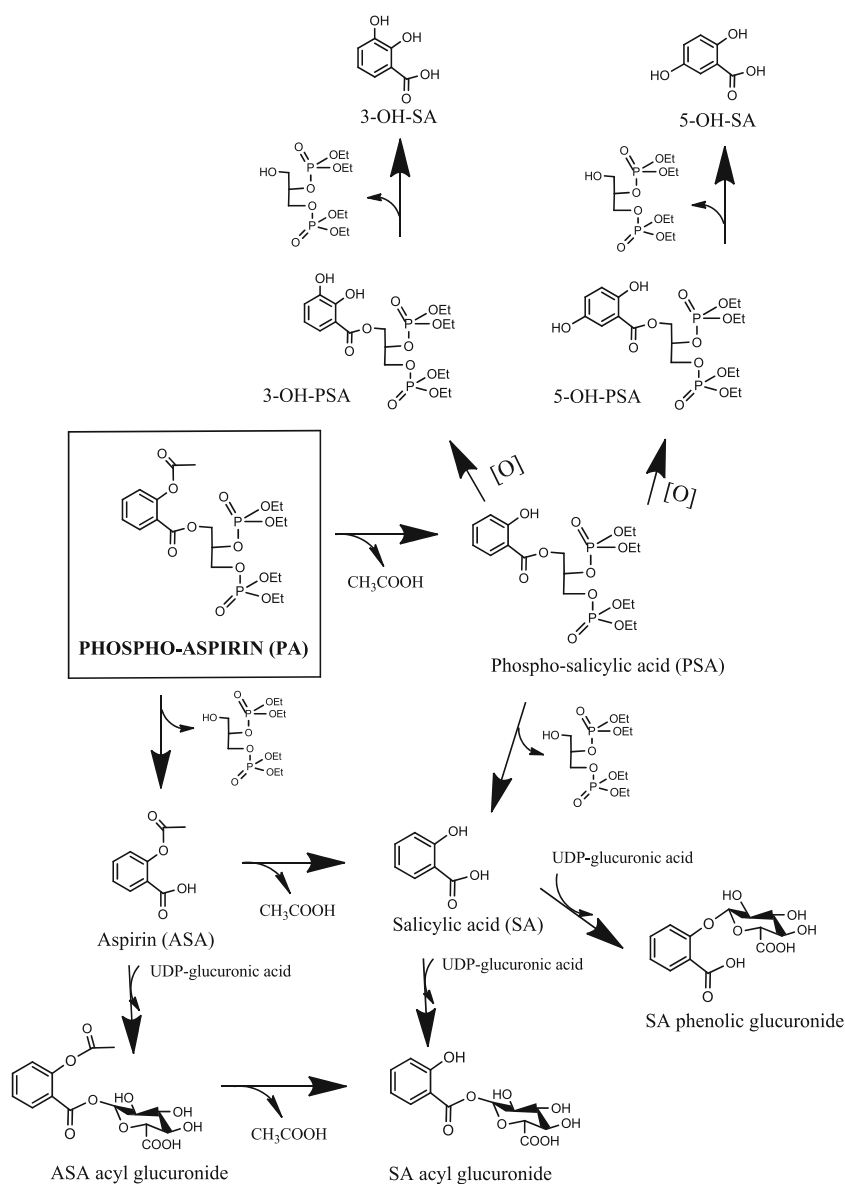


Fig. 7 Drug levels in PA- or ASA-treated rat plasma upon peroral administration. Equimolar PA or ASA at 0.2 mmol/kg in corn oil was administered to rats orally by gavage. Drug level in plasma was determined by HPLC, as described in Methods. * $P < 0.01$.

Fig. 8 The metabolic pathways of PA *in vitro* and *in vivo*. PA is rapidly deacetylated at its ASA moiety to form PSA. The resulting PSA undergoes regioselective oxidation to form 3-OH-PSA and 5-OH-PSA, which can be hydrolyzed to release 5-OH-SA and 3-OH-SA, respectively. PA also can be hydrolyzed at its carboxylic ester bond to release ASA, which can then be deacetylated to form SA. ASA and SA can be glucuronidated to form their acyl glucuronides. SA also can form its phenolic glucuronide.



constituents attenuated its anti-cancer potency (16). Non-specific carboxylic ester hydrolases are classified into acetylsterases, carboxylesterases and arylersterases based on their substrate specificity. Definitions of these enzymes support that acetylsterases primarily catalyze the deacetylation of PA to PSA, whereas carboxylesterases catalyze the hydrolysis of the carboxylic ester bond.

Deacetylation of PA to PSA is a rapid process, essentially accounting for the instability of PA. PA was far more stable in human liver and intestinal microsomes compared to those from mouse and rat, due to the slower deacetylation in human microsomes. PA was deacetylated more rapidly in MLM than RLM, but the opposite was true in intestinal microsomes. These results reflect the differences in isoform composition and expression of acetylsterases among different species and organs, as previously shown (17,18).

Compared to the deacetylation of PA, hydrolysis at its carboxylic ester bond is much slower. This is also reflected in our observation that ASA (in contrast to PSA) was undetectable in PA-treated liver microsomes. There are two major isoforms of carboxylesterases (CES), CES1 and

Table III Comparison of Lipophilicity of PA and its Metabolites

| | LogP | HPLC Retention Time, min |
|-----|------|--------------------------|
| PA | 3.5 | 10.2 |
| PSA | 3.7 | 10.8 |
| ASA | 1.2 | 7.1 |
| SA | 2.3 | 8.0 |

LogP (P is octanol-water partition coefficient) is determined using ChemDraw 7.0

CES2, with complementary substrate selectivity. CES1 hydrolyzes esters with a large acyl moiety, whereas CES2 hydrolyzes those with a small acyl group. Consistent with this notion, the hydrolysis of PA at its carboxylic ester bond is attributed essentially to CES2 (16). Thus, the strong CES2 expression in mouse liver (19) likely accounts for the potent hydrolysis of the carboxylic ester bond in MLM.

PSA also undergoes CYP-mediated regioselective hydroxylation at its SA moiety, which is far more rapid in MLM and RLM than HLM. Its minimal oxidation in HLM is reflected by the activity and selectivity of PSA oxidation by human CYPs. CYP2C19 and 2D6, the active isoforms towards PSA, account for only 4% and 2% of the total CYPs in human liver, respectively (20). It will be of interest to further identify which CYP isoforms in mouse and rat liver efficiently oxidize PSA.

In contrast to PSA, conventional SA and ASA were not appreciably oxidized by CYPs in liver microsomes, indicating that PSA is a preferred substrate of CYPs. PSA is more lipophilic than SA and ASA (Table III); substrate lipophilicity is highly correlated with their binding affinity to CYPs (21). The altered acidity of PSA is another critical factor to its binding by CYPs, as CYPs generally prefer neutral or basic substrates (22). Thus, the phospho-modification promotes the binding of PSA to CYPs by enhancing its lipophilicity and masking the -COOH group.

PA, in contrast to PSA, cannot be directly oxidized by CYPs in liver microsomes, indicating that the acetyl group of PA abrogates its oxidation by CYPs. We propose that the acetyl group of PA induces steric hindrance and blocks the access of PA to the active site of CYP. In support of this hypothesis, it has been shown that the acetylene group of butylphenylacetylene abrogates CYP-mediated oxidation by steric hindrance (23).

Glucuronidation plays an important role in the detoxification and elimination of lipophilic xenobiotics (24). While SA can be glucuronidated at its free -COOH and phenolic -OH groups, PA cannot. Glucuronidation is an S_N2 reaction in which a nucleophilic substrate attacks the electrophilic C-1 atom of glucuronic acid (25). The free -COOH and phenolic -OH groups of SA are both acidic and easily deprotonated to form anions, which act as strong nucleophiles in S_N2 reactions.

The metabolic fate of PA has important implications for its efficacy and safety. Given the strong carboxylesterase activity in rodents, it is not surprising that intact PA or PSA could not be detected following the oral administration of PA in rats. Interestingly, it has been shown that carboxylesterase activity is much lower in human blood than in mouse or rat blood (26). It is conceivable that PA would be considerably more stable in human liver, intestine and blood compared to the corresponding ones from mouse or rat. Since intact PA possesses a greater anticancer activity than

its hydrolysis products (16), the higher stability of PA in humans may lead to even stronger anti-cancer efficacy compared to that in laboratory rodents.

On the other hand, equimolar doses of PA generated over 3-fold lower levels of SA in rat plasma compared to ASA. Thus, PA reduces the systemic exposure of SA in blood, which is a favorable factor in terms of safety. Furthermore, the high susceptibility of PSA to CYP-mediated oxidation in microsomes supports its rapid clearance and detoxification *in vivo*, which likely contributes to the improved safety of PA (9).

CONCLUSIONS

PA undergoes extensive metabolic transformations *in vitro* and *in vivo*, generating an array of metabolites. Our results reveal significant inter-species differences in PA metabolism, and provide an insight into the interactions of PA and its metabolites with CYPs.

ACKNOWLEDGMENTS AND DISCLOSURES

This work was supported by the Department of Defense grant W81XWH1010873 and National Institute of Health grant 5R01CA139454-03. We also thank R. Rieger and T. Koller, Stony Brook University, for their expert LC-MS/MS analysis of our samples and the shared instrumentation grant, NIH/NCRR 1S10 RR023680-1.

The authors have nothing to disclose except for BR, who has an equity position in Medicon Pharmaceuticals, Inc., and PPC who is affiliated with the same.

REFERENCES

- Shimmura K, Kodani E, Xuan YT, Dawn B, Tang XL, Bolli R. Effect of aspirin on late preconditioning against myocardial stunning in conscious rabbits. *J Am Coll Cardiol.* 2003;41:1183–94.
- Corley DA, Kerlikowske K, Verma R, Buffler P. Protective association of aspirin/NSAIDs and esophageal cancer: a systematic review and meta-analysis. *Gastroenterology.* 2003;124:47–56.
- Hanif R, Pittas A, Feng Y, Koutsos MI, Qiao L, Staiano-Coico L, Shiff SI, Rigas B. Effects of nonsteroidal anti-inflammatory drugs on proliferation and on induction of apoptosis in colon cancer cells by a prostaglandin-independent pathway. *Biochem Pharmacol.* 1996;52:237–45.
- Iglesias-Serret D, Pique M, Barragan M, Cosialls AM, Santidrian AF, Gonzalez-Girones DM, Coll-Mulet L, de Frias M, Pons G, Gil J. Aspirin induces apoptosis in human leukemia cells independently of NF-kappaB and MAPKs through alteration of the Mcl-1/Noxa balance. *Apoptosis: an International Journal on Programmed Cell Death.* 2010;15:219–29.
- Borthwick GM, Johnson AS, Partington M, Burn J, Wilson R, Arthur HM. Therapeutic levels of aspirin and salicylate directly inhibit a model of angiogenesis through a Cox-independent mechanism. *The FASEB journal: official publication of the Federation*

- of American Societies for Experimental Biology. 2006;20:2009–16.
6. Dube C, Rostom A, Lewin G, Tsertsvadze A, Barrowman N, Code C, Sampson M, Moher D. The use of aspirin for primary prevention of colorectal cancer: a systematic review prepared for the U.S. Preventive Services Task Force. *Annals of Internal Medicine*. 2007;146:365–75.
 7. Baigent C, Blackwell L, Collins R, Emberson J, Godwin J, Peto R, Buring J, Hennekens C, Kearney P, Meade T, Patrono C, Roncaglioni MC, Zanchetti A. Aspirin in the primary and secondary prevention of vascular disease: collaborative meta-analysis of individual participant data from randomised trials. *Lancet*. 2009;373:1849–60.
 8. Hochgesang GP, Rowlinson SW, Marnett LJ. Tyrosine-385 is critical for acetylation of cyclooxygenase-2 by aspirin. *J Am Chem Soc*. 2000;122:6514–5.
 9. Huang L, Mackenzie G, Ouyang N, Sun Y, Xie G, Johnson F, Komninou D, Rigas B. The novel phospho-non-steroidal anti-inflammatory drugs, OXT-328, MDC-22 and MDC-917, inhibit adjuvant-induced arthritis in rats. *Br J Pharmacol*. 2011;162:1521–33.
 10. Huang L, Mackenzie GG, Sun Y, Ouyang N, Xie G, Vrankova K, Komninou D, Rigas B. Chemotherapeutic properties of phosphonosteroidal anti-inflammatory drugs, a new class of anticancer compounds. *Cancer Res*. 2011;71:7617–27.
 11. Liu D, Zheng X, Tang Y, Zi J, Nan Y, Wang S, Xiao C, Zhu J, Chen C. Metabolism of tanshinol borneol ester in rat and human liver microsomes. *Drug Metabolism and Disposition: the Biological Fate of Chemicals*. 2010;38:1464–70.
 12. Damre A, Mallurwar SR, Behera D. Preparation and characterization of rodent intestinal microsomes: comparative assessment of two methods. *Indian Journal of Pharmaceutical Sciences*. 2009;71:75–7.
 13. Rao CV, Joseph S, Gao L, Patlolla JM, Choi CI, Kopelovich L, Steele VE, Rigas B. Pharmacokinetic and pharmacodynamic study of NO-donating aspirin in F344 rats. *Int J Oncol*. 2008;33:799–805.
 14. Xie G, Sun Y, Nie T, Mackenzie GG, Huang L, Kopelovich L, Komninou D, Rigas B. Phospho-ibuprofen (MDC-917) is a novel agent against colon cancer: efficacy, metabolism, and pharmacokinetics in mouse models. *J Pharmacol Exp Ther*. 2011;337:876–86.
 15. Xie G, Nie T, Mackenzie G, Sun Y, Huang L, Ouyang N, Alston N, Zhu C, Murray O, Constantinides P, Kopelovich L, Rigas B. The metabolism and pharmacokinetics of phospho-sulindac (OXT-328) and the effect of difluoromethylornithine. *Br J Pharmacol*. 2012;165:2152–66.
 16. Wong CC, Cheng KW, Xie G, Zhou D, Zhu CH, Constantinides PP, Rigas B. Carboxylesterases 1 and 2 hydrolyze phosphonosteroidal anti-inflammatory drugs: relevance to their pharmacological activity. *J Pharmacol Exp Ther*. 2012;340:422–32.
 17. Holmesand RS, Masters CJ. The developmental multiplicity and isoenzyme status of rat esterases. *Biochim Biophys Acta*. 1967;146:138–50.
 18. Holmesand RS, Masters CJ. A comparative study of the multiplicity of mammalian esterases. *Biochim Biophys Acta*. 1968;151:147–58.
 19. Hosokawa M. Structure and catalytic properties of carboxylesterase isozymes involved in metabolic activation of prodrugs. *Molecules*. 2008;13:412–31.
 20. Pelkonen O, Maenpaa J, Taavitsainen P, Rautio A, Raunio H. Inhibition and induction of human cytochrome P450 (CYP) enzymes. *Xenobiotica; the Fate of Foreign Compounds in Biological Systems*. 1998;28:1203–53.
 21. Lewis DF, Jacobs MN, Dickens M. Compound lipophilicity for substrate binding to human P450s in drug metabolism. *Drug Discovery Today*. 2004;9:530–7.
 22. Lewis DF. On the recognition of mammalian microsomal cytochrome P450 substrates and their characteristics: towards the prediction of human p450 substrate specificity and metabolism. *Biochem Pharmacol*. 2000;60:293–306.
 23. Zhang H, Lin HL, Walker VJ, Hamdane D, Hollenberg PF. tert-Butylphenylacetylene is a potent mechanism-based inactivator of cytochrome P450 2B4: inhibition of cytochrome P450 catalysis by steric hindrance. *Mol Pharmacol*. 2009;76:1011–8.
 24. Kuehl GE, Lampe JW, Potter JD, Bigler J. Glucuronidation of nonsteroidal anti-inflammatory drugs: identifying the enzymes responsible in human liver microsomes. *Drug Metabolism and Disposition: the Biological Fate of Chemicals*. 2005;33:1027–35.
 25. Mulder GJ. Glucuronidation and its role in regulation of biological activity of drugs. *Annu Rev Pharmacol Toxicol*. 1992;32:25–49.
 26. Li B, Sedlacek M, Manoharan I, Boopathy R, Duysen EG, Masson P, Lockridge O. Butyrylcholinesterase, paraoxonase, and albumin esterase, but not carboxylesterase, are present in human plasma. *Biochem Pharmacol*. 2005;70:1673–84.